

Extreme wave analysis for marine renewable energies in Ireland

Nahia Martinez-Iturricastillo ^{a,b} ,* , Meábh Nic Guidhir ^c  , Alain Ulazia ^d  , John V. Ringwood ^a 

^a Centre for Ocean Energy Research, Maynooth University, Maynooth, Co. Kildare, Ireland

^b Hamilton Institute, Maynooth University, Maynooth, Co. Kildare, Ireland

^c Met Éireann, D09 Y921 Dublin, Ireland

^d Energy Engineering Department, University of the Basque Country (UPV/EHU), Otaola 29, 20600 Eibar, Spain

ARTICLE INFO

Keywords:

Extreme waves
Marine renewable technologies
Offshore wind
Cluster analysis
ERA5
Buoy data
Reanalysis data

ABSTRACT

The characterization of extreme wave climates and future projection analyses are essential for offshore renewable energy planning and coastal protection. This study examines the maximum individual wave height (H_{max}) around Ireland, using ERA5 reanalysis data from 1991 to 2020, validated against H_{max} observations from Irish moored buoys. Extreme wave climate regions are defined, employing a model-based clustering technique, which relies on the wave height distribution of each area. The probability of rogue waves – defined as waves where the maximum wave height is at least twice the significant wave height – is assessed for each region. The results suggest that, while extreme waves are more likely to occur far offshore on the west coast of Ireland, the likelihood of rogue waves is higher on the east coast and closer to shore. The Gumbel distribution is employed to estimate the 50-year return period H_{max} values; these projections are compared to the National Renewable Energy Laboratory's threshold of 30 m, representing the maximum 50-year return period wave height offshore wind turbines must withstand. This threshold is exceeded in areas far offshore from Ireland's west coast, particularly near the M6 buoy location. Additional analyses of thresholds, at 29 and 28 m, suggest a broader area may be impacted by these high waves. The findings provide valuable insights into the spatial variability of extreme wave events, informing risk assessments for offshore renewable energy developments.

1. Introduction

The significance of wave energy and floating offshore wind energy, in the future energy landscape, cannot be overstated. As the global demand for sustainable energy sources intensifies, both wave and floating wind energy present viable solutions to address this challenge under the expected evolution due to future climate change [1]. Wave energy, characterized by its high energy density and predictability, offers a reliable and consistent power generation source, which is relevant for stabilizing energy supplies, especially in coastal regions [2]. The potential for wave energy is substantial, with estimates suggesting it could meet a significant portion of global energy needs, particularly in areas with favourable oceanographic conditions [3,4]. Furthermore, the development of advanced wave energy converters (WECs) allows energy to be harvested in deeper waters, thus expanding the commercial scope for energy production [5].

On the other hand, floating offshore wind energy is gaining traction, as a complementary technology to traditional wind energy sources. The ability to deploy floating wind turbines in deeper waters, where wind speeds are typically higher and more consistent, enhances their

efficiency and output [6]. Studies indicate that floating offshore wind farms can significantly contribute to energy resilience and reliability, especially when integrated with other renewable sources, such as solar energy [7] or wave energy [8]. The economic feasibility of these technologies is also improving, with ongoing research focusing on reducing the levelized cost of electricity (LCoE) associated with floating wind systems [9].

Moreover, the synergy between wave and wind energy systems can lead to optimized energy production, as their generation profiles often complement each other, thus maximizing the overall output from marine renewable resources [10,11]. In conclusion, the future of energy generation will likely be shaped by the integration of wave energy and floating offshore wind energy, both of which offer unique advantages that can help meet the growing energy demands while promoting sustainability and reducing carbon emissions [12].

Extreme wave event analysis is crucial for the design and operation of the mentioned marine renewable energy (MRE) systems, such as offshore wind turbines, wave energy converters, and tidal energy devices. These systems are exposed to highly dynamic and unpredictable

* Corresponding author at: Hamilton Institute, Maynooth University, Maynooth, Co. Kildare, Ireland.
E-mail address: nmiturri@gmail.com (N. Martinez-Iturricastillo).

List of abbreviations

ERA5	Fifth generation ECMWF atmospheric reanalysis
WEC	Wave Energy Converter
LCoE	Levelized Cost of Energy
MRE	Marine Renewable Energy
UK	United Kingdom
ORESS	Offshore Renewable Electricity Support Scheme
NREL	National Renewable Energy Laboratory
IMDBON	Irish Marine Data Buoy Observation Network
ECMWF	European Centre for Medium-Range Weather Forecasts
GP	Grid Point
RMS	Root-mean-square
GMM	Gaussian Mixture Model
EM	Expectation Maximization
BIC	Bayes Information Criterion
GEV	Generalized Extreme Value
RP	Return period

List of nomenclature

H_{max}	Maximum individual wave height
H_s	Significant wave height
RW_r	Rogue wave ratio

ocean conditions, including extreme wave events, which can result from storms, rogue waves, or long-term climate variability [13–15]. Such events can cause significant structural stress, fatigue, or even catastrophic failure of MRE devices, even in paradigmatic areas such as the study area of this article in Ireland [16,17]. In this respect, the West of Ireland is a referential location, due to the complementary high wind and wave energy potential [18–20], but the presence of extreme events presents challenges to system survival [21,22].

By analysing wave height, period, and direction during extreme conditions, engineers can develop more resilient structures, optimize energy production, and ensure the safety and longevity of MRE installations. Additionally, this analysis informs risk assessment and maintenance planning, contributing to the sustainability of marine renewable energy projects, which is an important point rarely studied in the literature [23]. To the best of the authors' knowledge, this is a first attempt to analyse this risk assessment, using maximum individual wave height data from real data buoys combined with reanalysis data, which can offer a better approximation to rogue waves and extreme wave impact on MRE systems.

1.1. Literature review

The characterization of wave climate is a topic of interest for many researchers, with long-term significant wave height changes being studied globally. For example, [24] compares the long term trends of mean significant wave height between four different datasets, satellite altimeter products, reanalysis and hindcast products. The effect of such trends on wave energy has also been explored [19,25,26].

Extreme waves have also been studied, [27], reviewing the impacts of climate change in storms and waves around the United Kingdom. The need to analyse extreme climate is highlighted for sustainable development of coastal and offshore infrastructure, as well as for management of coastal resources and ecosystems. [28] for example, employs long term buoy measurements to analyse the relationship between maximum individual wave height and significant wave height during storms off the coast of Portugal.

Future wave climate projections, such as those articulated by the Coordinated Ocean Wave Climate Projections (COWCLIP), do not include maximum individual wave height values; rather, they provide

significant wave height (H_s) projections, while significant wave height has been used in the literature [29,30] to assess extreme wave conditions. [31] creates a summary for extreme significant wave height statistics, based on significant wave height thresholds. [32] investigates the changes in global 100-year return period significant wave height, employing an ensemble approach to reduce the uncertainty of projections and concluding that, in the North Atlantic, at low to mid latitudes, there is a projected decrease in significant wave height while, at high latitudes, there is an increase. [33] analyses the influence of large-scale atmospheric oscillations on the wave and wind climate in the Northeast Atlantic, around Ireland, with correlations between those oscillations and the 95th percentile significant wave height analysed.

Extreme waves presents various risks, such as infrastructure damage, coastal flooding, or other environmental impacts. In this regard, [34] classifies global coastlines in terms of storminess level. [35] conducts a comprehensive study to assess the coastal flooding risk in Dublin, Ireland, considering the impacts of climate change, sea level rise, and extreme storm events. The findings highlight the significant role of extreme waves and storm surges in exacerbating coastal flooding, since these events force water into coastal areas, leading to higher and more frequent inundation. [36] performs an analysis on extreme storm-wave events across the United Kingdom, employing significant wave height data from buoy observation. The focus is on assessing coastal flood risk, extreme buoy observations are clustered in regions to understand the spatial extent of each storm, with the temporal aspect also analysed. With regard to marine renewable technologies, combined extreme wind and wave loads present a risk to the foundations of fixed offshore wind turbines [37], but also need to be accounted for in floating offshore wind turbines [38,39].

Due to its geographical location, storms and extreme waves are not uncommon in Ireland. Various researchers have analysed extreme wave events in Ireland. [40] creates an exhaustive catalogue of extreme wave events in Ireland from 14 680 before present to 2017. Additionally, [41] conducts an analysis of a rogue wave, recorded by Irish weather buoys, where a maximum individual wave height of 32.3 m was observed in October 2020 off the west of Ireland.

1.2. Objectives and paper layout

This paper aims to analyse the spatial distribution of extreme waves in the eastern north Atlantic, specifically around Ireland. The objectives are as follows: (i) to define regions around Ireland with similar extreme wave distributions; (ii) to assess the probability of rogue waves in each region and, (iii) to analyse historical records of extreme waves and future extreme wave projections, calculated using Generalized Extreme Value (GEV) theory, to identify critical areas for offshore wind planning.

The remainder of this paper is organized as follows: Section 2 describes the data sources, along with the validation statistical indices and diagrams used in the analysis. Section 3 presents the main methodology, including cluster analysis for identifying H_{max} climate regions in Ireland, while the Gumbel distribution is defined for return period analysis, the limit waves for referential wind turbines are described, and the nature of rogue waves is also explained. Finally, Section 4 presents the results, conclusions are drawn in Section 5 with the main outcomes, as well as the limitations, highlighted.

2. Data

2.1. Study area

Ireland is the first landmass between the North Atlantic Ocean and Continental Europe, which endows it with strong wave and wind resources, due to prevailing westerly winds [42]. Consequently, marine renewable technologies have the capability to significantly contribute to Ireland's energy mix. In 2023, the Irish government held its first

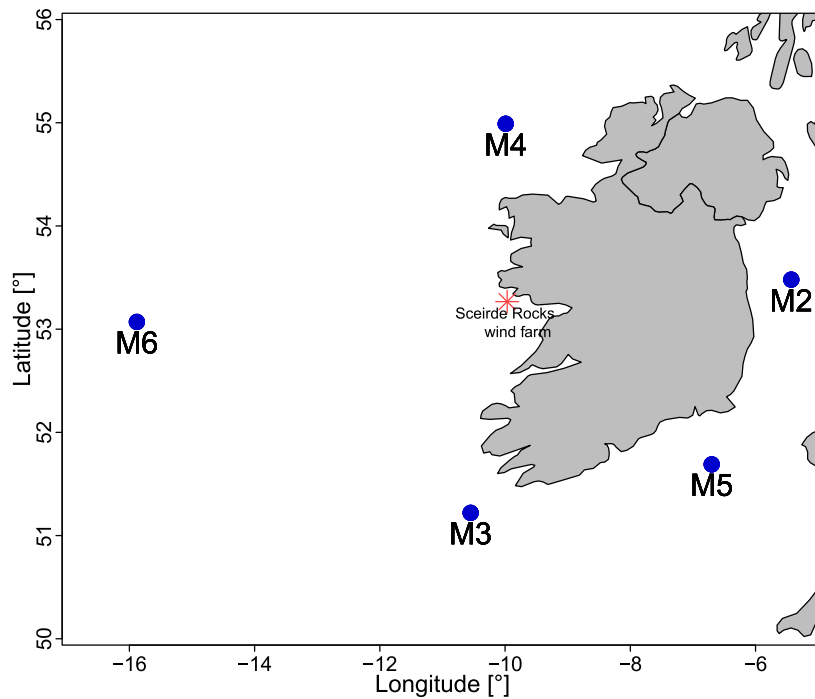


Fig. 1. Area of study around Ireland. The location of IMDBON buoys is marked with blue dots, and the location of the first offshore wind project approved for the West coast of Ireland is marked with a red star.

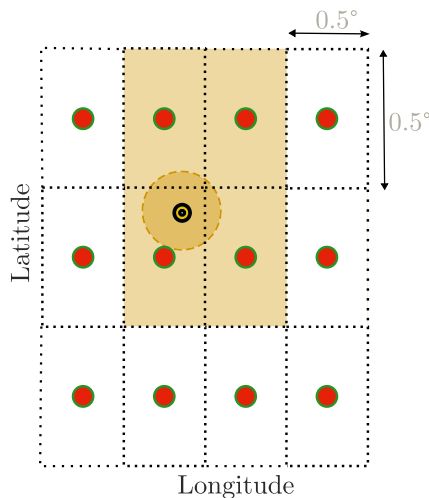


Fig. 2. Graphical representation of ERA5 spatial resolution and GP considered for validation. The buoy is represented by a black, with an inner yellow–black–blue dot. ERA5 grid-points are green-red dots, with a spatial resolution of 0.5°. The large orange area around the buoy represents the 15 km region surrounding the buoy. The orange squares enclose the GPs that are inside the red circle and therefore the average value of the GPs inside this orange square are compared against the buoy for validation. (For interpretation of the references to colour in this figure legend, the reader is referred to the web version of this article.)

offshore wind auction, accepting projects with a combined capacity of 3074 MW. The only accepted project on the West Coast, highlighted in Fig. 1, is a 450 MW fixed offshore wind turbine project, with construction scheduled to begin in 2026. Additionally, the results for the ORESS 2.1 auction are expected in 2025, with an additional 900 MW of capacity to be auctioned for installation along Ireland’s South West Coast [43].

In the context of offshore wind energy development in Ireland, [44] performed an exhaustive analysis on offshore wind site selection for the Republic of Ireland, based on the LCoE, but wave climate was

Table 1

Dates at which the IMDBON were upgraded; the dates correspond to the first recorded observation for the new generation buoy. The M6 buoy was upgraded directly from the first to the third generation, as the second-generation buoys were not robust enough to withstand the challenging environmental conditions at the M6 location.

Buoy	First generation	Second generation	Third generation
M2	03-May-2001 14:00:00	23-Feb-2011 07:00:00	07-Mar-2022 08:00:00
M4	15-Apr-2003 11:00:00	07-Jun-2011 08:00:00	15-Jul-2020 18:00:00
M3	22-Jul-2002 08:00:00	31-May-2012 14:00:00	23-Oct-2020 10:00:00
M5	18-Oct-2004 10:00:00	21-Feb-2012 13:00:00	22-Jan-2020 13:00:00
M6	25-Sep-2006 09:00:00	NA	01-Jun-2019 00:00:00

not accounted for, nor extreme ocean waves. Previous studies analysed rogue waves in Ireland, employing buoy data [41]. This article analyses the extreme wave climate in Ireland, the analysed area being shown in Fig. 1, with a goal of defining regions with relatively homogeneous climatic conditions as well as regions where the 50-year return period H_{max} surpasses the 30 m limit established by the National Renewable Energy Laboratory (NREL).

2.2. Irish buoys

The Irish Marine Data Buoy Observation Network (IMDBON), managed by the Marine Institute and Met Éireann, measures wave data alongside other environmental parameters. However, due to the relatively short duration of the dataset, it cannot be used alone to evaluate long-term wave climate trends. The IMDBON network has five buoys, the locations of which are identified in Fig. 1. Initially deployed in the early 2000s, the network is now in its third generation of buoys. In terms of ocean wave characteristics, the first generation buoys measured non-directional parameters only (i.e.: significant wave height and mean wave period). From the second generation onward, additional wave features have been recorded, such as the mean wave direction or the maximum individual wave height [41]. The dates when each buoy was upgraded are listed in Table 1.

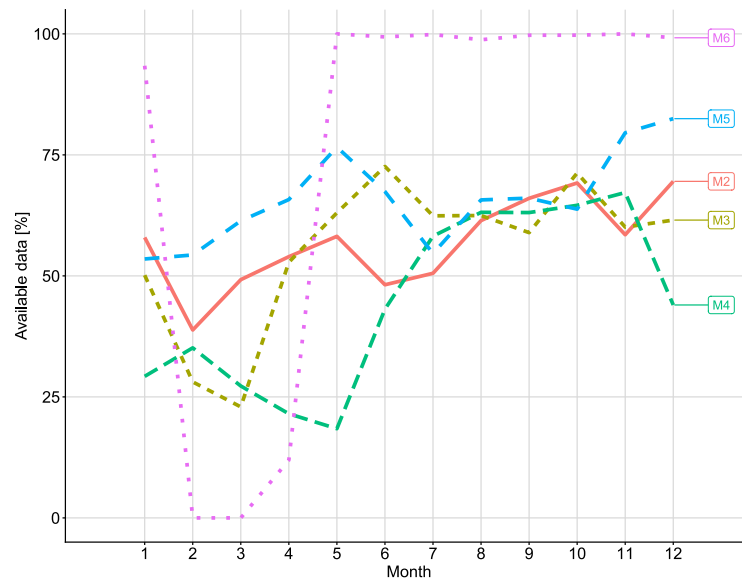


Fig. 3. Percentage of hourly available H_{max} observations, per IMDBON buoy, from the first recorded measurement until December 2020.

2.3. ERA5 reanalysis

ERA5 is a global atmospheric reanalysis dataset produced by the European Centre for Medium-Range Weather Forecasts (ECMWF) [45]. It provides a high-resolution long-term dataset of atmospheric and oceanographic variables such as temperature, pressure, wind, humidity, and precipitation [46]. ERA5 is created using a complex assimilation system, that combines observations from various sources with a state-of-the-art atmospheric model, to produce a consistent and comprehensive dataset. This reanalysis is widely used by scientists and researchers for climate studies, weather forecasting, and understanding atmospheric processes, together with wind and wave energy studies [47]. ERA5 data provides measurements on a grid, with a spatial resolution of 0.5° for ocean waves and 0.25° for atmospheric variables. The temporal resolution is 1-h, and data is available from 1940 to the present [45].

In this article, maximum individual wave height (H_{max}), together with significant wave height (H_s), are employed for extreme event analysis.

2.4. Validation

To assess the utility of the ERA5 dataset for wave climate analysis around Ireland, a comparative analysis between the IMDBON wave data and the ERA5 dataset over the past 10 years is performed. For validation purposes, an area around each buoy is defined, within which the values of the grid points (GPs) are averaged and then compared to the buoy measurements. This area extends radially from each buoy to a distance of 15 km. The way those areas are defined is represented in Fig. 2: The buoy appears as a black dot with an inner yellow–black–blue dot, while the GPs are shown as green, red dots. Each GP is represented within a dotted square, indicating its area of influence. The light brown circle around the buoy marks the 15 km region, and the rectangle in that shade of colour encloses the GPs within this region. The averaged values of the GPs inside this brown rectangle are then compared to the buoy measurements for validation.

Taylor diagrams are a powerful visualization tool, used to assess the performance of models against observational data [48]. They plot correlation coefficients, standard deviation, and root-mean-square (RMS) difference in polar coordinates, providing a comprehensive overview of model accuracy and relationship to observed data. Models closer to the origin have better agreement, while those closer to unity correlation

have a stronger positive linear relationship. Taylor diagrams are widely used in fields such as meteorology, climatology, and hydrology for model evaluation, data comparison, and sensitivity analysis.

The variation of each individual time series is assessed by the standard deviation, which is quantified by the radial distance from the dots to the origin. The distance from the origin to the reference point in the x -axis represents the standard deviation of the reference dataset (buoy data); the standard deviation of reanalysis data is represented by the radial distance of the other dot, which also quantifies the correlation and RMS difference. The correlation is represented by the angle from the x axis, with points closer to the x -axis indicating higher correlation. The RMS difference is represented by concentric circles centred on the reference point, with closer points indicating a lower RMS difference.

The distribution of each pair of time series is also compared through box plots, where quartiles are visually represented.

3. Methodology

3.1. Cluster analysis

Cluster analysis is a technique employed to investigate the underlying structure of the data. Clustering algorithms have been previously used by researchers to study spatial distributions of precipitation, temperature and air pollution [49–52]. Clustering has also been employed to analyse wave climate and wave energy resources [53,54]. In the current article, locations with similar extreme wave distributions around Ireland are grouped or clustered.

K-means is a widely used clustering algorithm, which assumes all observations belong uniquely to a specific group, and known as *hard clustering*. In contrast, the analysis presented in the current paper employs Gaussian Mixture Models (GMMs) to define regions of extreme wave climate around Ireland. GMMs are, in contrast, a *soft clustering* technique, where each observation is assigned a probability of belonging to a specific group [55].

Distributions of H_{max} are spatially clustered using the historical information over the study period (1991–2020), forming regions with similar features, to understand the extreme wave climate patterns around Ireland. More precisely, the cluster method assumes that daily H_{max} , denoted by $\mathbf{X} = (X_1, \dots, X_t)$ where t are the number of days, follows a mixture of multivariate normal distributions with K the

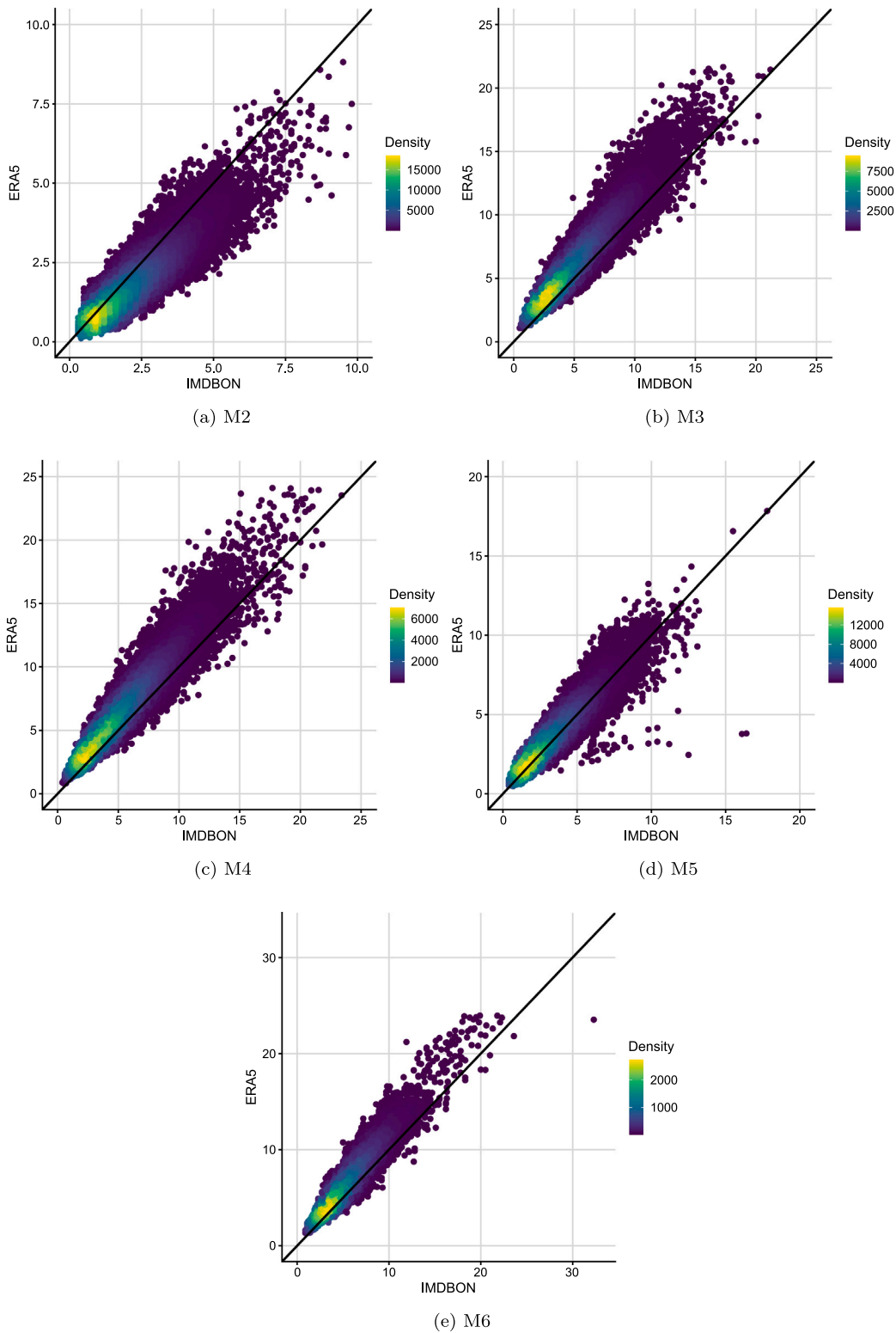


Fig. 4. ERA5 vs. IMDBON correlation plots, the colour of the points represent the amount of observations in that area, a brighter colour meaning more observations. The black diagonal line represents perfect correlation, i.e. $IMDBON = ERA5$. (For interpretation of the references to colour in this figure legend, the reader is referred to the web version of this article.)

number of components. Then, the joint probability density of \mathbf{X} is defined by

$$p(\mathbf{x} | \boldsymbol{\pi}, \boldsymbol{\mu}, \boldsymbol{\Sigma}) = \sum_{k=1}^K \pi_k f_k(\mathbf{x} | \boldsymbol{\mu}_k, \boldsymbol{\Sigma}_k), \tag{1}$$

where $f_k(\mathbf{x}; \boldsymbol{\mu}_k, \boldsymbol{\Sigma}_k)$ denotes the density of the k th component $\mathcal{N}(\mathbf{x}; \boldsymbol{\mu}_k, \boldsymbol{\Sigma}_k)$, π_k is the probability that an observation (\mathbf{x}) is generated by the k th component, with $\pi_k \geq 0$ for $k = 1, \dots, K$, and $\sum_{k=1}^K \pi_k = 1$.

Using the observed historical H_{max} samples for each grid point, denoted by $\mathbf{x}_i = (x_{i1}, \dots, x_{is})$ for $i = 1 \dots, N$, with N being the number

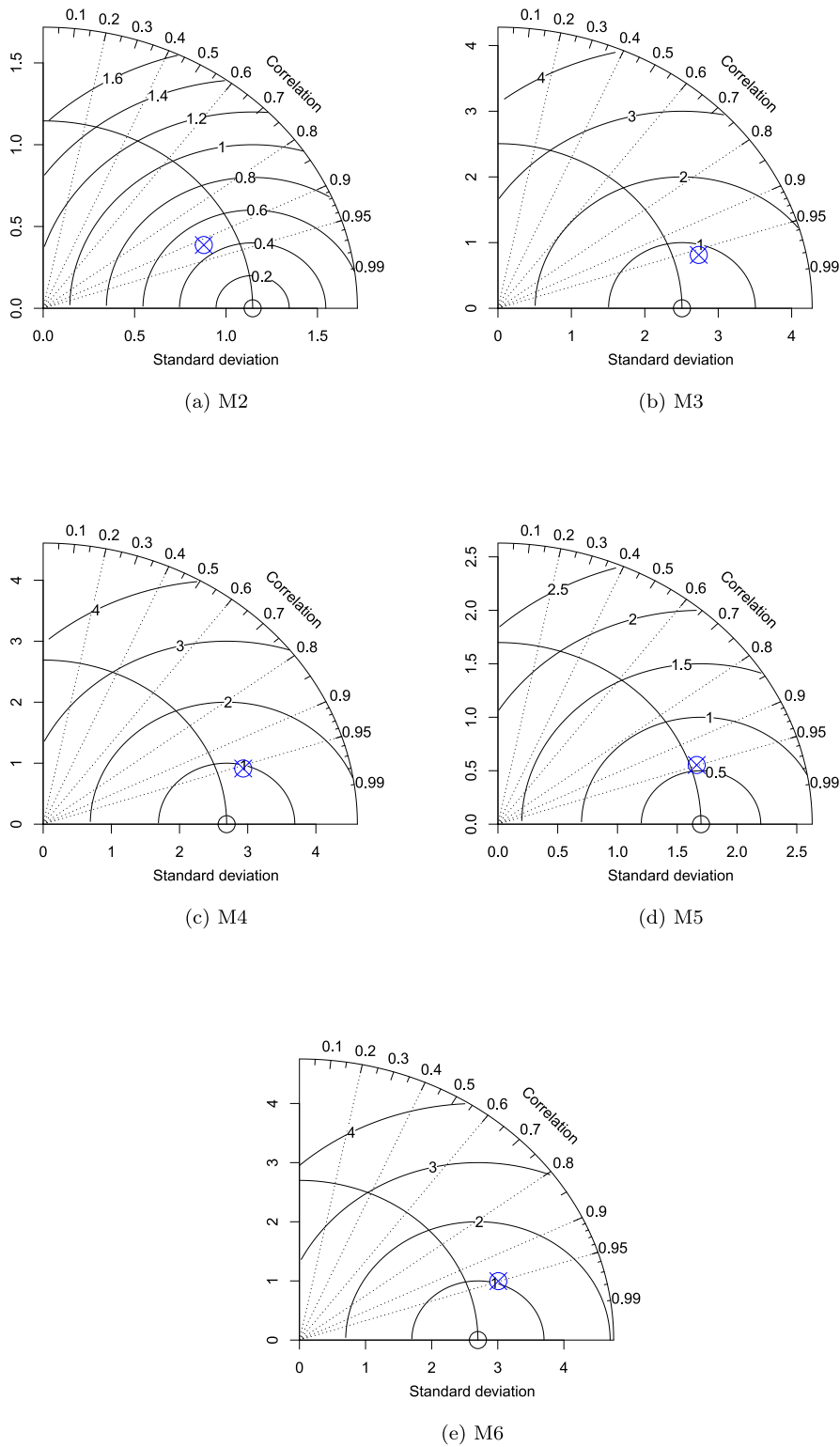


Fig. 5. Taylor diagrams, comparison between buoy observations and ERA5 data for each buoy. The black dot represents the standard deviation of the buoy time series. The blue dot represent the standard deviation of ERA5, as well as the correlation and root mean square (RMS) difference between both time series.

of grid points, the model parameters, $\theta = (\pi, \mu, \Sigma)$, are estimated using the Expectation Maximization (EM) algorithm. Due parsimony, $K = 3$ is considered since with $K > 3$, many specific groups are observed in coastal areas, leading to difficult interpretation of the clusters. Clustering analysis is performed, using a model-based clustering technique

implemented in R package *mclust* [56], which chooses the model based on the lowest Bayes Information Criterion (BIC). The multivariate models employed in this analysis are VII (all year, winter and summer), EVI (autumn), and EEI (spring) [57].

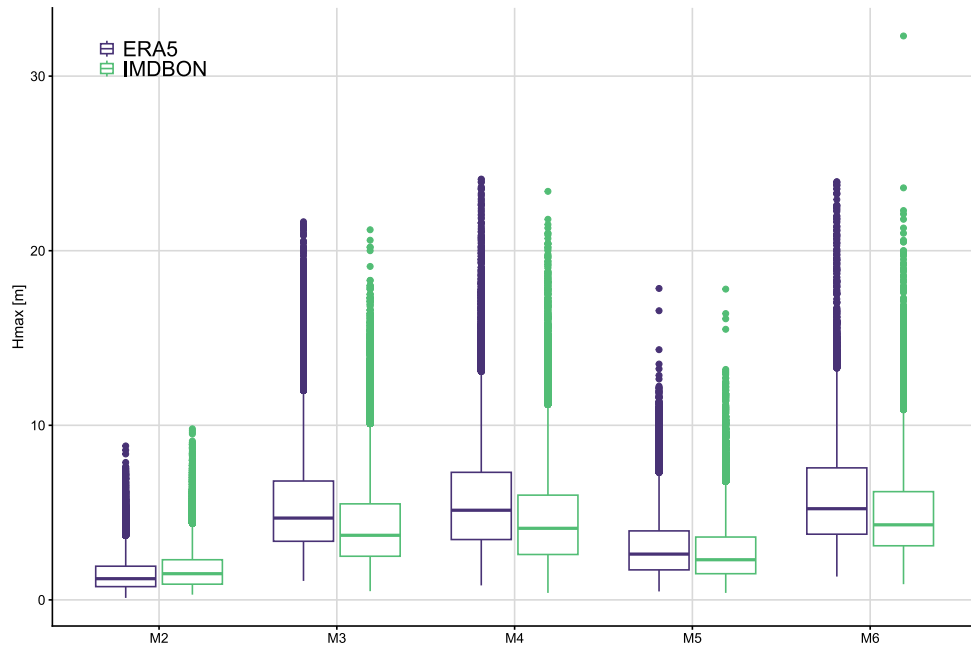


Fig. 6. Distribution of the time series of each buoy for ERA5 reanalysis data and IMDBON observations. (For interpretation of the references to colour in this figure legend, the reader is referred to the web version of this article.)

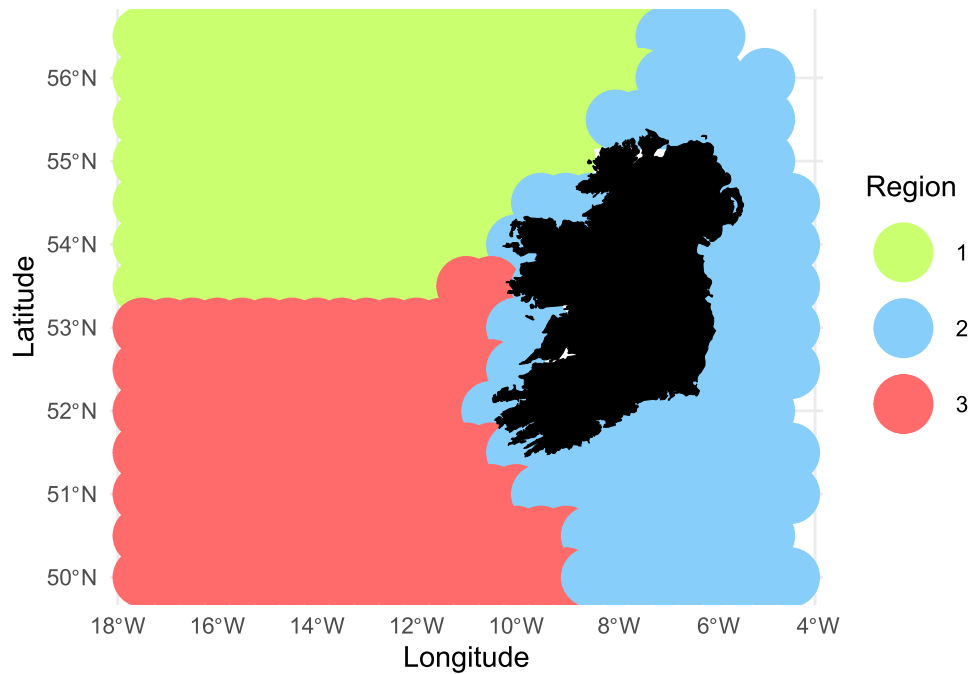


Fig. 7. Three main H_{max} climate regions around Ireland, across the area in which all weather buoys are installed. Climate regions are inferred by the cluster technique described in Section 3.1. The main features of each region are presented in Table 2. (For interpretation of the references to colour in this figure legend, the reader is referred to the web version of this article.)

3.2. Generalized extreme value distribution

Return period levels are common practice in climate studies, as well as in engineering [33,52,54,58]. They represent the probability of an event happening over a specific duration, based on past data. A 50-year return period means that there is a ($\frac{1}{50} = 0.02$) %2 probability of that event happening in any given year.

To calculate the predicted nominal wave height to be exceeded in the future, yearly maxima H_{max} are employed to calculate the return

H_{max} for each ERA5 GP on the analysed area around Ireland. These values are derived from hourly data.

The Generalized Extreme Value (GEV) distribution is applied for this purpose. This distribution, defined in Eq. (2), depends on three parameters: shape (μ), location (σ), and scale (ξ):

$$G(z) = \exp \left(- \left[1 + \xi \left(\frac{z - \mu}{\sigma} \right) \right]^{-1/\xi} \right). \tag{2}$$

Once the parameters are fitted to the data, the distribution can be inverted to determine the M – year return levels, which represent the H_{max} expected to be exceeded every M years. The probability of

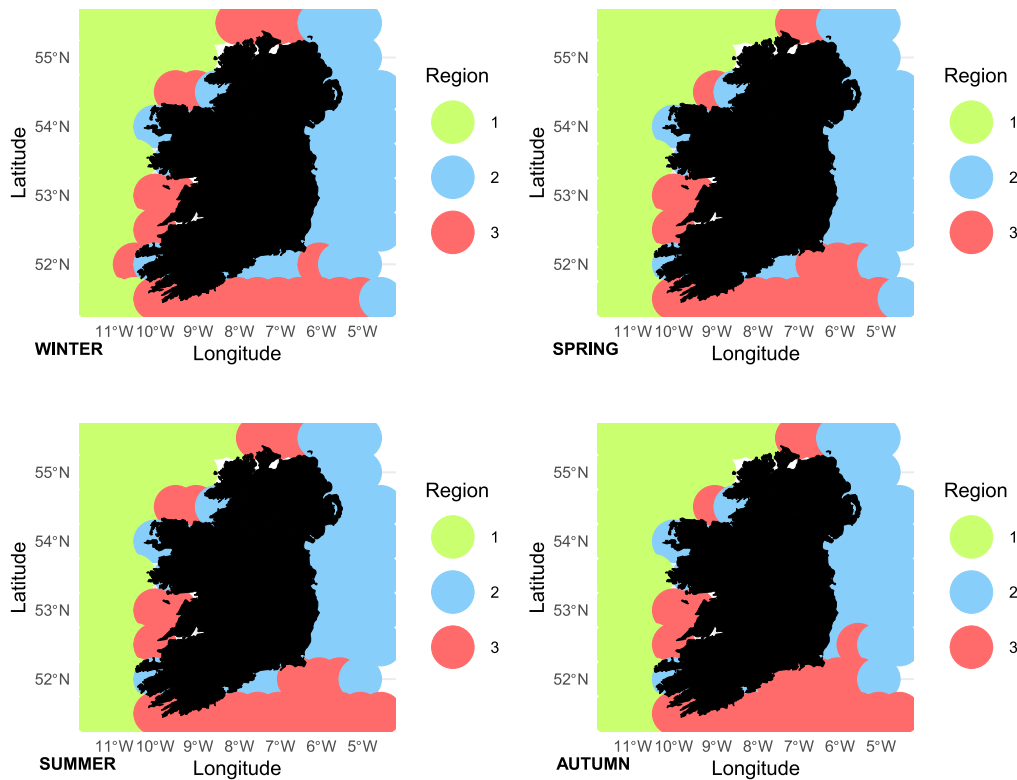


Fig. 8. Three main H_{max} climate regions around Ireland per season for the nearshore area (the longitudinal space is limited to 11.5°W). Climate regions are inferred by the cluster technique described in Section 3.1. The main features of each region are presented in Table 3. (For interpretation of the references to colour in this figure legend, the reader is referred to the web version of this article.)

exceeding this value in any given year are $1/M$. For this analysis, $M = 50$, as the 50-year return period H_{max} is calculated for each ERA5 grid point.

The GEV distribution parameters are estimated using *ismev* R package [59], which employs maximum likelihood estimation for parameter fitting.

3.3. Limit waves for offshore wind turbines

The NREL report on the 5-MW reference wind turbine, designed for offshore applications, establishes a reference wave height limit for offshore wind turbines [58]. It specifically states that the NREL 5-MW baseline turbine was developed to evaluate offshore wind technologies, including floating platforms in deep waters. The maximum wave height considered for this turbine is 30 m, which represents a 50-year return period wave event. This corresponds to a wave amplitude of 15 m, ensuring that the turbine can withstand harsh ocean conditions. Additionally, the IEC-61400-3 standard, which specifies the design requirements for offshore wind turbines, mandates that an offshore wind turbine must withstand the 50-year extreme wave height. 50-year return period wave height means that there is a 2% chance of exceeding that in any given year.

3.4. Rogue wave ratio

A rogue wave ratio ($RW_r = H_{max}/H_s > 2$) value greater than 2 indicates a wave that is significantly larger than the average wave height in a given area. This is a defining characteristic of rogue waves, which are exceptionally large and unpredictable waves that can pose serious threats to marine vessels and coastal structures [60,61]. $RW_r > 2$ signifies a wave that is significantly taller than the surrounding waves, making it a potential rogue wave. Rogue waves are notoriously difficult to predict, as they can appear suddenly and without warning,

even in relatively calm seas. These waves can pose serious risks to ships, offshore platforms, and coastal infrastructure. The factors [62] contributing to rogue waves are:

- Rogue waves can arise from nonlinear interactions between waves, leading to constructive interference and the formation of exceptionally large crests.
- Strong currents can focus wave energy, increasing the likelihood of rogue wave formation.
- Severe weather events, such as hurricanes or storms, can generate large waves and increase the risk of rogue waves.

While $RW_r > 2$ is a strong indicator of a potentially dangerous wave, it is important to note that other factors, such as the wave period and steepness, can also influence its impact.

4. Results

4.1. Data analysis

The variable of interest for this study is maximum individual wave height (H_{max}), and the validation of ERA5 against IMDBON is performed from 2011 until 2020. After the data cleaning process, there is an average of 57.20% of the IMDBON data available. This percentage varies per month, and is lower in the winter season, when outages are more likely due to more extreme storms and reduced solar power generation. The available data, per month and buoy, are shown in Fig. 3.

4.2. Validation of ERA5 versus buoys

As explained in Section 2, buoy observations are compared to ERA5 values for validation. To achieve this, ERA5 grid points within a 15 km radius of the buoy are averaged. The selected area for this calculation

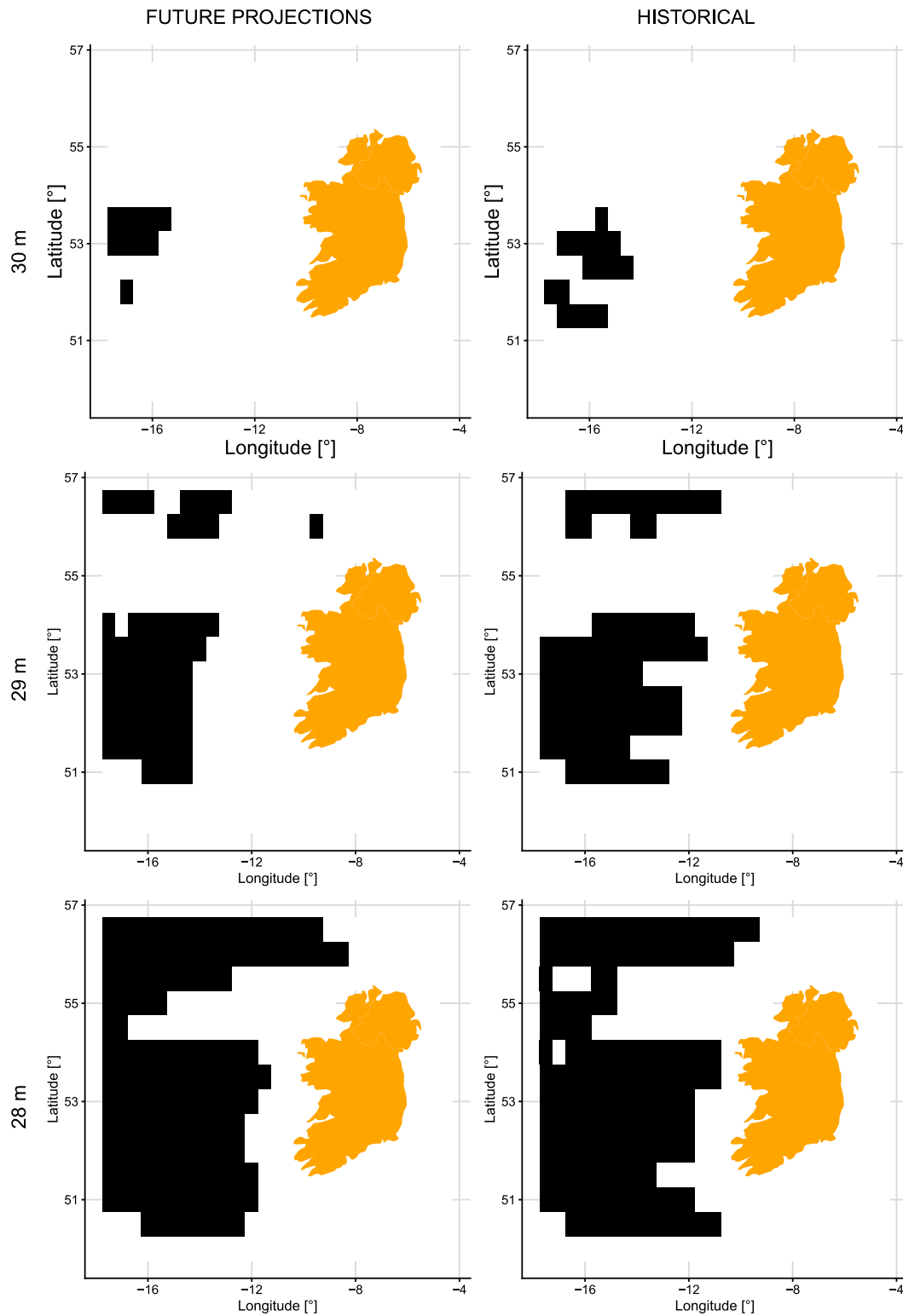


Fig. 9. H_{max} thresholds and scenarios. The panels in the top row correspond to 30-m waves, the middle row to 29-m waves, and the bottom row to 28-m waves. The left panes represent future projections, calculated via the 50-year return period analysis, while the right panes represent historical data analysis (1991–2020). Black grid cells represent areas where the maximum wave height limit is exceeded, in each scenario.

is illustrated schematically in Fig. 2. The correlation between the buoy observations and ERA5 reanalysis data, for each buoy, is presented in Fig. 4, where the black line represents perfect linear correlation.

Taylor diagrams, in Fig. 5, are polar plots that show the standard deviation of each individual time series (IMDBON and ERA5), as explained in greater detail in Section 2.4. The correlation between buoy

and reanalysis data exceeds 0.9 for all buoys. The RMS difference is close to or below unity, which is represented by the concentric circles in the plot. The standard deviations of buoy and reanalysis time series are represented by the horizontal and vertical axes; which are identical since it is a polar plot. The radial distance from the origin represents the standard deviation. The variation in both time series is similar.

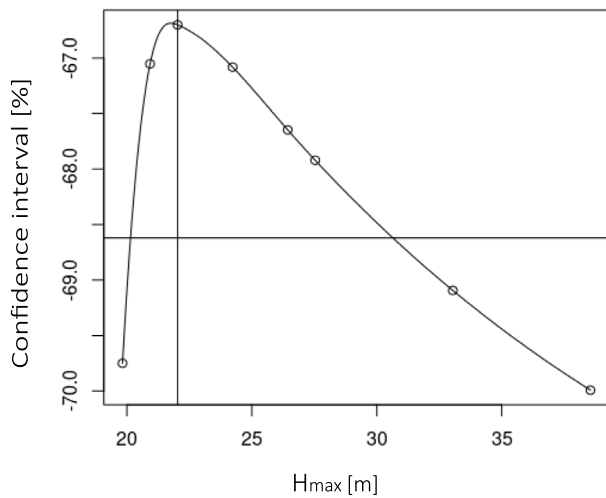


Fig. 10. Confidence interval for a return period of 100 years, in which there is a narrow probability to surpass the 30 m extreme wave. The GEV likelihood is reparameterized in terms of the unknown return level (H_{max}) and profile likelihood arguments (vertical axis) are used to construct a confidence interval.

Table 2

Summary statistics for the three regions presented in Fig. 7, across the area in which all weather buoys are installed. Daily observations of H_{max} from 1991 to 2020 are used, without seasonal classification. Regions are inferred by the cluster technique described in Section 3.1.

Region	# GP	Min	25%	Median	Mean	75%	95%	99%	Max
1	123	0.85	4.51	6.51	7.28	9.22	14.39	18.77	30.01
2	94	0.05	2.05	3.29	3.88	5.07	8.91	12.28	25.48
3	113	0.85	4.35	6.19	6.97	8.78	13.80	17.99	30.47

The boxplots, in Fig. 6, show that the ERA5 data tends to overestimate extreme wave heights. Although the interquartile ranges are similar, both the 25% and 75% quartiles are higher compared to the buoy data. This is also perceived in the scatterplots in Fig. 4, where observations lay above the perfect correlation line. In the case of M2 buoy, both the scatterplot and boxplot show the opposite, that buoy values are higher than the reanalysis data, this could be attributed to the area chosen for averaging the reanalysis observations, as the M2 buoy is closer to shore than the other buoys, and consequently, the averaging area is also closer to shore.

Overall, a strong agreement between the two datasets is observed, with correlations above 0.9 and similar distributions.

4.3. Regions according to cluster analysis

Daily maxima H_{max} are employed to define the climatic extreme wave regions around Ireland. Data spanning from 1991 to 2020 are employed from ERA5 reanalysis, covering a total of 330 grid points within the area defined by longitude $[-17.5, -4.5]$ and latitude $[50, 56.5]$. An initial analysis is performed using all available data, with results presented in Fig. 7 and Table 2.

To gain further insight into the nearshore areas and seasonal variations, the longitudinal range is narrowed, and regions are analysed by season, as shown in Fig. 8 and Table 3. The seasons are defined as follows: winter (December–January–February), spring (March–April–May), summer (June–July–August), and autumn (September–October–November), following the meteorological definition.

With the data partitioned spatially as in Fig. 7, it is seen that the area closer to shore and eastern parts of the domain comprise a single region, whereas the deeper water in the western part of the domain is divided into northern and southern regions. Following a closer look at the summary statistics for each region, it is clear that both regions

in the deeper Atlantic Ocean have similar features. Therefore, in order to gain more insight into the extreme wave climate closer to Ireland, the longitude dimension is reduced and the regions are redefined, as presented in Fig. 8 and Table 3, with the longitudinal dimension reduced and regions defined per season.

Fig. 8 offers a distinct perspective on the climatic extreme wave regions around Ireland, compared to the previous analysis in Fig. 7. Grid points are grouped, based on similarities in their extreme wave distributions. Consequently, the Irish Sea, the Atlantic Ocean, and the South East Coast are divided into separate regions. Notably, some GPs along the West Coast of Ireland are not classified within the Atlantic Ocean region; this may be due to their proximity to the shore, and/or shallower bathymetry.

Overall, each GP remain within the same region throughout the year. However, both wave distribution and wave height exhibit substantial variability across seasons, as illustrated in Table 3. It is also noteworthy that there is a considerable difference between the overall maximum H_{max} and the 99th percentile, with an even larger gap when compared to the 95th percentile. This indicates that these extreme waves are outliers, lying firmly within the tail of the distribution.

4.4. Wave height limit for offshore wind turbines

The NREL baseline for offshore wind turbines defines the maximum 50-year return period wave height as 30 m [58]. To assess Ireland’s suitability for wind farm development, the 50-year return period wave height is calculated for each individual grid point. This calculation uses the annual maximum wave height (H_{max}) and applies generalized extreme value theory, as explained in Section 3.2.

The expected maximum wave height for 2070 is calculated. In Fig. 9, projected maximum wave heights are compared with historical records side by side, with areas where the maximum wave height is exceeded highlighted in black. The wave height limit for each row of paired plots is set at 30, 29, and 28 m, respectively.

The 30-m wave height limit has already been surpassed in the North Atlantic Ocean to the west of Ireland, as shown in Fig. 9B. This area includes the location of the M6 buoy from the IMDBON, situated approximately 400 km from shore. Projections indicate that the 30-m wave height limit will also be exceeded in this area by 2070. In contrast, the 29 and 28 m wave height projections cover a broader region across the North Atlantic Ocean, as seen in Fig. 9C and E, respectively. Historical ERA5 reanalysis data confirm that wave heights of 29 and 28 m have already occurred closer to the Irish shoreline, covering an even larger area of the Atlantic Ocean, as illustrated in Fig. 9D and F.

4.5. Confidence intervals

In practical applications, such as the analysis of extreme meteorological events, the Gumbel distribution’s confidence bounds can be critical. Chun et al. [63] illustrate that, while the Gumbel distribution can adequately capture extreme events, confidence bounds derived from normal approximations may fail to encompass these events, highlighting the necessity for robust statistical methods. This emphasizes the need for careful consideration of the underlying distribution when estimating confidence intervals, particularly in extreme value contexts.

Table 4 shows Gumbel distribution parameter estimates, and their associated 95% confidence intervals, for return levels at 25, 50, 75, 100, 125 and 150-year return periods, derived from ERA5 H_{max} data, for the nearest grid point to the offshore wind project ($10^{\circ}W, 53^{\circ}N$) near Galway, pinpointed in Fig. 1. The 50 year return period (RP) superior limit is around 27 m, 75 year RP exceeds 29 m, and 100 years is the limit to expect an interval superior limit with waves above 30 m. However, the inferior limit barely exceeds 20 m, even for a 150 year RP.

The asymmetry between the slow increment of the inferior limit of the confidence interval with RP and the higher expansion of the superior limit with respect to the central value is shown in Fig. 10, in which the values for 100 year RP is drawn.

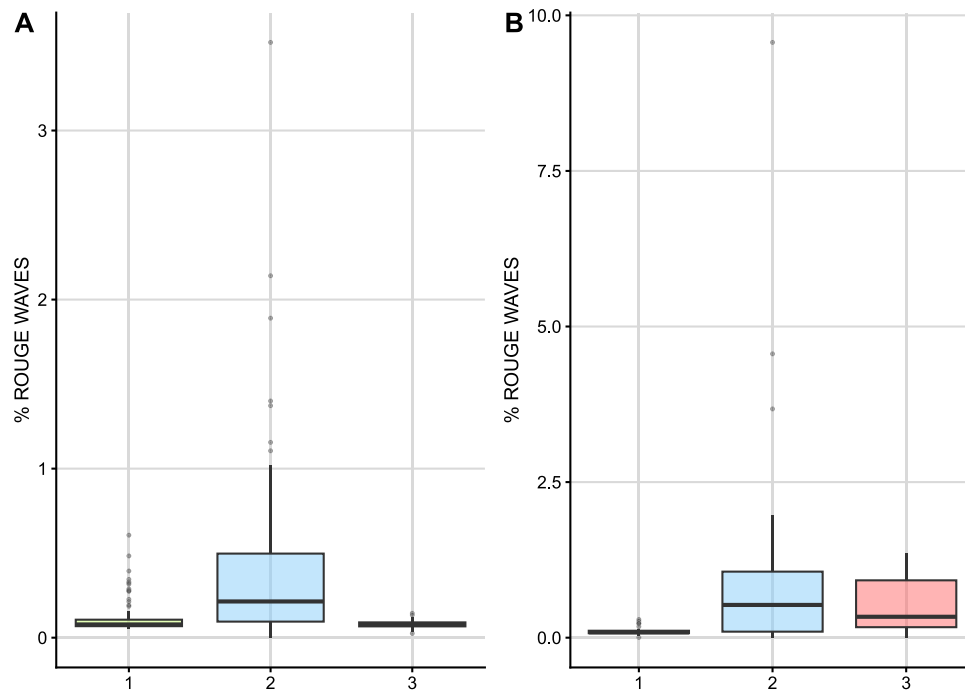


Fig. 11. Distribution of probability of occurrence of rogue waves per cluster. On the left (A), the distribution of rogue waves corresponding to the regions defined in Fig. 7. On the right (B), the distribution of rogue waves corresponding to the regions defined in Fig. 8-winter. Rogue waves are more likely to happen close to shore and in winter.

Table 3

Summary statistics for the three regions presented in Fig. 8, the longitudinal space is limited to 11.5°W. Daily observations of H_{max} from 1991 to 2020 are employed for each season. Regions are inferred by the cluster technique described in Section 3.1.

Season	Region	# GP	Min	25%	Median	Mean	75%	95%	99%	Max
Winter	1	34	0.25	3.36	5.70	6.730	9.14	15.90	21.15	29.05
	2	37	0.29	2.48	4.17	4.86	6.52	10.61	16.66	22.46
	3	22	0.52	3.34	5.53	6.23	8.46	13.34	18.73	22.82
Spring	1	38	0.28	2.36	3.83	4.38	5.53	9.95	16.16	18.30
	2	35	0.29	2.30	3.83	4.38	5.62	9.60	17.23	19.04
	3	20	0.52	3.34	5.54	6.51	8.76	5.37	6.25	7.12
Summer	1	36	0.33	1.73	2.55	2.76	3.58	5.40	7.13	8.54
	2	34	0.35	2.07	3.16	3.54	4.64	7.34	9.66	14.02
	3	23	0.25	1.90	3.12	3.31	4.48	6.92	8.59	10.46
Autumn	1	38	0.18	2.02	3.71	4.57	6.53	10.95	14.31	16.16
	2	31	0.54	3.37	5.27	6.09	8.26	12.87	16.53	17.99
	3	24	0.39	3.06	5.34	5.83	8.29	12.14	15.42	17.20

Table 4

H_{max} confidence intervals (inferior, central, and superior value at 95%), according to a Gumbel distribution with return periods ranging from 25 to 150 years. The analysed location corresponds to the nearest ERA5 GP to the accepted offshore wind project starred in Fig. 1.

RP (years)	inf(H_{max}) (m)	central(H_{max}) (m)	sup(H_{max}) (m)
25	18.92	20.28	24.42
50	19.62	21.20	27.32
75	19.98	21.69	29.14
100	20.20	22.03	30.65
125	20.34	22.28	31.76
150	20.42	22.48	32.72

4.6. Probability of occurrence of rogue waves

In order to analyse the probability of occurrence of rogue waves, a comparison between H_s and H_{max} is performed. ERA5 reanalysis hourly data from 1991–2020 is employed to assess whether the ratio between H_s and H_{max} exceeds two, as explained in Section 3.4. The total number of hours in which this threshold of two is exceeded is calculated, along with the percentage of hours for each GP. Fig.

11 displays the distribution of rogue wave occurrence probability by cluster, corresponding to the regions outlined in Figs. 7 and 8 (Winter). Fig. 11 presents the probability of rogue wave occurrence, defined as instances where H_{max} is at least twice H_s , displayed by region or cluster. The left plot indicates that rogue waves are more likely to occur closer to shore, with Region 2 showing a particularly high probability of occurrence. The right plot, which focuses on winter months, shows an increased likelihood of rogue waves, especially at nearshore grid points in Regions 2 and 3.

5. Conclusions

To the best of our knowledge, this is the first analysis using H_{max} data from real buoys and reanalysis for extreme events and definition of extreme wave climate regions. The North Atlantic Ocean plays an important role in defining the wave climate in Ireland and, on closer inspection, the West Coast of Ireland experiences smaller waves compared to far offshore, as shown in Table 2. Cluster analysis shows that regions remain consistent throughout the year, even if the scale of extreme waves fluctuates, as shown in Fig. 8 and Table 3.

Regarding offshore wind limits on extreme waves, it is noteworthy that the 30-m (NREL) threshold has historically been surpassed, even

though this occurs far from shore, specifically near the M6 buoy located at 16°W longitude. The area where the 28-m extreme wave limit has been recorded is broader, encompassing most of the west coast of Ireland, at 110 km to the South West Coast of County Kerry and 50 km to County Mayo in the North West. Consequently, the results suggest that, following current offshore wind turbine certification limits, wind farm developments would not be suitable in very far-offshore areas to the West of Ireland.

The rogue wave analysis, on the other hand, indicates that rogue waves are more likely to occur closer to shore. This implies that, even if significant wave heights are more modest in the nearshore, higher individual waves are expected more frequently. Such findings should be considered in the planning and development of marine renewable technologies, such as offshore wind farms or wave energy converters.

5.1. Limitations and reproducibility

The methodology presented in this paper defines extreme wave climate regions and identifies areas potentially unsuitable for marine renewable energy planning, based on current wave limits and offshore wind turbine standards. This approach is replicable to other geographic locations and can be updated in the future with newer data or evolving certification requirements.

5.2. Future research

Future research could analyse the distribution of H_{max} per region, and assess monthly variability and the possible effect of climate change. This would provide a clearer understanding of the temporal and spatial variability of extreme wave heights, which is crucial for the planning and design of marine renewable energy projects. Furthermore, how different marine renewable energy requirements would affect the thresholds and affected areas could be investigated. This includes examining the impact of varying turbine standards, wave energy converter designs, and other technological advancements on the suitability of different regions for marine renewable energy development in Ireland.

CRediT authorship contribution statement

Nahia Martínez-Iturricastillo: Writing – review & editing, Writing – original draft, Visualization, Validation, Software, Resources, Project administration, Methodology, Investigation, Funding acquisition, Formal analysis, Data curation, Conceptualization. **Meábh Nic Guidhir:** Writing – review & editing, Supervision, Project administration, Conceptualization. **Alain Ulazia:** Writing – review & editing, Writing – original draft, Visualization, Supervision, Formal analysis, Conceptualization. **John V. Ringwood:** Writing – review & editing, Supervision.

Declaration of competing interest

The authors declare that they have no known competing financial interests or personal relationships that could have appeared to influence the work reported in this paper.

Acknowledgements

The IMDBON network is managed by the Marine Institute in collaboration with Met Éireann and funded by the Department of Agriculture, Food and the Marine.

This publication has emanated from research supported in part by a grant from Taighde Éireann – Research Ireland under Grant number 18/CRT/6049. For the purpose of Open Access, the author has applied a CC BY public copyright licence to any Author Accepted Manuscript version arising from this submission. This paper is part of project PID2020-116153RB-I00 funded by MCIN/AEI/10.13039/501100011033, and also received funding from the University of Basque Country (UPV/EHU project GIU20/008). Support was also received through the SFI Centre for Energy, Climate and Marine research and innovation (MaREI) under Grant 12/RC/2302 P2.

Data availability

The datasets employed are available online. ERA5 data was downloaded from Copernicus website. Wave buoy data can be downloaded from the Marine Institute website.

References

- [1] Ibarra-Berastegui G, Sáenz J, Ulazia A, Sáenz-Aguirre A, Esnaola G. CMIP6 projections for global offshore wind and wave energy production (2015–2100). *Sci Rep* 2023;13(1):18046.
- [2] Douziech F, et al. Are wave and tidal energy plants new green technologies? *Environ Sci Technol* 2016;50(16):8831–40.
- [3] Qiao Y, et al. Review of wave energy converter and design of mooring system. *Sustain* 2020;12(19):8251.
- [4] Aderinto A, Li Y. Ocean wave energy converters: Status and challenges. *Energies* 2018;11(5):1250.
- [5] Guo B, Ringwood JV. A review of wave energy technology from a research and commercial perspective. *IET Renew Power Gener* 2021;15(14):3065–90.
- [6] Pham T, et al. Prospects and economics of offshore wind turbine systems. *J Ocean Eng Technol* 2021;35(1):1–12.
- [7] Beiter P, Musial W, Duffy P, Cooperman A, Shields M, Heimiller D, Optis M. The cost of floating offshore wind energy in California between 2019 and 2032 (No. NREL/TP-5000-77384). Tech. rep., Golden, CO (United States: National Renewable Energy Lab.(NREL); 2020.
- [8] Fusco F, Nolan G, Ringwood JV. Variability reduction through optimal combination of wind/wave resources - an Irish case study. *Energy* 2010;35(1):314–25.
- [9] Martínez A, Iglesias G. Mapping of the levelised cost of energy for floating offshore wind in the European Atlantic. *Renew Sustain Energy Rev* 2022;154:111889.
- [10] Ulazia A, Sáenz J, Ibarra-Berastegui G, González-Rojí SJ, Carreno-Madinabeitia S. Using 3DVAR data assimilation to measure offshore wind energy potential at different turbine heights in the West Mediterranean. *Appl Energy* 2017;208:1232–45.
- [11] Ulazia A, Sáenz J, Saenz-Aguirre A, Ibarra-Berastegui G, Carreno-Madinabeitia S. Paradigmatic case of long-term collocated wind-wave energy index trend in Canary Islands. *Energy Convers Manage* 2023;283:116890.
- [12] Raajiv R, Vijaya Kumar R, Pandey JK. Ocean energy—A myriad of opportunities in the renewable energy sector. *Clean Renew Energy Prod* 2024;225–46.
- [13] Johnson M, Lee S. Extreme wave analysis for the structural design of offshore wind turbines. *Renew Energy* 2023;178:345–59.
- [14] Saenz-Aguirre A, Fernandez-Gamiz U, Zulueta E, Aramendia I, Teso-Fz-Betono D. Flow control based 5 MW wind turbine enhanced energy production for hydrogen generation cost reduction. *Int J Hydrog Energy* 2022;47(11):7049–61.
- [15] Saenz-Aguirre A, Saenz J, Ulazia A, Ibarra-Berastegui G. Optimal strategies of deployment of far offshore co-located wind-wave energy farms. *Energy Convers Manage* 2022;251:114914.
- [16] Williams E, Green R. Risk assessment of marine renewable energy devices under extreme wave events. *J Ocean Eng Sci* 2022;45:112–25.
- [17] Ulazia A, Ezpeleta H, Ibarra-Berastegi G, Sáenz J, Martínez-Iturricastillo N, Ringwood JV. Historical trends of floating wind turbine fatigue loads (Ireland 1920–2010). *Ocean Eng* 2024;299:117424.
- [18] Gallagher S, Tiron R, Whelan E, Gleeson E, Dias F, McGrath R. The nearshore wind and wave energy potential of Ireland: a high resolution assessment of availability and accessibility. *Renew Energy* 2016;88:494–516.
- [19] Penalba M, Ulazia A, Ibarra-Berastegui G, Ringwood J, Sáenz J. Wave energy resource variation off the west coast of Ireland and its impact on realistic wave energy converters' power absorption. *Appl Energy* 2018;224:205–19.
- [20] Doddy Clarke E, Sweeney C, McDermott F, Griffin S, Correia JM, Nolan P, Cooke L. Climate change impacts on wind energy generation in Ireland. *Wind Energy* 2022;25(2):300–12.
- [21] Tiron R, Gallagher S, Gleeson E, Dias F, McGrath R. The future wave climate of Ireland: from averages to extremes. *Procedia IUTAM* 2015;17:40–6.
- [22] O'Brien L, Dudley JM, Dias F. Extreme wave events in Ireland: 14 680 BP–2012. *Nat Hazards Earth Syst Sci* 2013;13(3):625–48.
- [23] Barkanov E, Penalba M, Martínez A, Martínez-Perurena A, Zarketa-Astigarra A, Iglesias G. Evolution of the European offshore renewable energy resource under multiple climate change scenarios and forecasting horizons via CMIP6. *Energy Convers Manage* 2024;301:118058.
- [24] Timmermans B, Gommenginger C, Dodet G, Bidlot J-R. Global wave height trends and variability from new multitemporal satellite altimeter products, reanalyses, and wave buoys. *Geophys Res Lett* 2020;47(9):e2019GL086880.
- [25] Penalba M, Ulazia A, Sáenz J, Ringwood JV. Impact of long-term resource variations on wave energy farms: The Icelandic case. *Energy* 2020;192:116609.
- [26] Ulazia A, Penalba M, Rabanal A, Ibarra-Berastegi G, Ringwood J, Sáenz J. Historical evolution of the wave resource and energy production off the Chilean coast over the 20th century. *Energies* 2018;11(9):2289.

- [27] Wolf J, Woolf D, Bricheno L. Impacts of climate change on storms and waves relevant to the coastal and marine environment around the UK. *MCCIP Sci Rev* 2020;2020:132–57.
- [28] Oliveira TC, Neves MG, Fidalgo R, Esteves R. Variability of wave parameters and Hmax/Hs relationship under storm conditions offshore the portuguese continental coast. *Ocean Eng* 2018;153:10–22.
- [29] Li D, Feng J, Zhu Y, Staneva J, Qi J, Behrens A, Lee D, Min S-K, Yin B. Dynamical projections of the mean and extreme wave climate in the Bohai Sea, Yellow Sea and east China sea. *Front Mar Sci* 2022;9:844113.
- [30] Lobeto H, Menendez M, Losada LJ. Future behavior of wind wave extremes due to climate change. *Sci Rep* 2021;11(1):7869.
- [31] Morim J, Trenham C, Hemer M, Wang XL, Mori N, Casas-Prat M, Semedo A, Shimura T, Timmermans B, Camus P, et al. A global ensemble of ocean wave climate projections from CMIP5-driven models. *Sci Data* 2020;7(1):105.
- [32] Meucci A, Young IR, Hemer M, Kirezci E, Ranasinghe R. Projected 21st century changes in extreme wind-wave events. *Sci Adv* 2020;6(24):7295.
- [33] Gleeson E, Clancy C, Zubiate L, Janjić J, Gallagher S, Dias F. Teleconnections and extreme ocean states in the Northeast Atlantic ocean. *Adv Sci Res* 2019;16:11–29.
- [34] Lobeto H, Semedo A, Lemos G, Dastgheib A, Menendez M, Ranasinghe R, Bidlot J-R. Global coastal wave storminess. *Sci Rep* 2024;14(1):3726.
- [35] Paranunzio R, Guerrini M, Dwyer E, Alexander PJ, O'Dwyer B. Assessing coastal flood risk in a changing climate for Dublin, Ireland. *J Mar Sci Eng* 2022;10(11):1715.
- [36] Malagon Santos V, Haigh ID, Wahl T. Spatial and temporal clustering analysis of extreme wave events around the UK coastline. *J Mar Sci Eng* 2017;5(3):28.
- [37] Yu D, Ye J, Yin C. Dynamics of offshore wind turbine and its seabed foundation under combined wind-wave loading. *Ocean Eng* 2023;286:115624.
- [38] Ju S-H, Huang Y-C. Study on multiple wind turbines in a platform under extreme waves and wind loads. *Energy Convers Manage: X* 2025;25:100877.
- [39] Ha K, Kim J-B, Yu Y, Seo H-S. Structural modeling and failure assessment of spar-type substructure for 5 MW floating offshore wind turbine under extreme conditions in the east sea. *Energies* 2021;14(20):6571.
- [40] O'Brien L, Renzi E, Dudley JM, Clancy C, Dias F. Catalogue of extreme wave events in Ireland: revised and updated for 14680 BP to 2017. *Nat Hazards Earth Syst Sci* 2018;18(3):729–58.
- [41] Nic Guidhir M, Kennedy D, Berry A, Christy B, Clancy C, Creamer C, Westbrook G, Gallagher S. Irish wave data—Rogues, analysis and continuity. *J Mar Sci Eng* 2022;10(8):1073.
- [42] Gaughan E, Fitzgerald B. An assessment of the potential for co-located offshore wind and wave farms in Ireland. *Energy* 2020;200:117526.
- [43] van Rensburg TM, Brennan N. Understanding public preferences towards Ireland's offshore wind sector: A study on renewable energy trade, public involvement, and setback distance. *Mar Policy* 2024;160:105988.
- [44] Martínez A, Iglesias G. Site selection of floating offshore wind through the levelised cost of energy: A case study in Ireland. *Energy Convers Manage* 2022;266:115802.
- [45] Hersbach H, Bell B, Berrisford P, Hirahara S, Horányi A, Muñoz-Sabater J, Nicolas J, Peubey C, Radu R, Schepers D, et al. The ERA5 global reanalysis. *Q J R Meteorol Soc* 2020;146(730):1999–2049.
- [46] Changing the reference period from 1981–2010 to 1991–2020 for the C3S climate bulletin. 2021.
- [47] Olauson J. ERA5: The new champion of wind power modelling? *Renew Energy* 2018;126:322–31.
- [48] Taylor KE. Summarizing multiple aspects of model performance in a single diagram. *J Geophys Res: Atmos* 2001;106(D7):7183–92.
- [49] Carvalho M, Melo-Gonçalves P, Teixeira J, Rocha A. Regionalization of europe based on a K-Means cluster analysis of the climate change of temperatures and precipitation. *Phys Chem Earth Parts A/ B/ C* 2016;94:22–8, 3rd International Conference on Ecohydrology, Soil and Climate Change, EcoHCC'14.
- [50] Govender P, Sivakumar V. Application of k-means and hierarchical clustering techniques for analysis of air pollution: A review (1980–2019). *Atmospheric Pollut Res* 2020;11(1):40–56.
- [51] Manuel G, Scotto SMB, Alonso AM. Extreme value and cluster analysis of European daily temperature series. *J Appl Stat* 2011;38(12):2793–804.
- [52] Elizabeth A. Maharaj AMA, D'Urso P. Clustering seasonal time series using extreme value analysis: An application to Spanish temperature time series. *Commun Stat: Case Stud Data Anal Appl* 2015;1(4):175–91.
- [53] Camus P, Mendez FJ, Medina R, Cofiño AS. Analysis of clustering and selection algorithms for the study of multivariate wave climate. *Coast Eng* 2011;58(6):453–62.
- [54] Fairley I, Lewis M, Robertson B, Hemer M, Masters I, Horrillo-Caraballo J, Karunaratna H, Reeve DE. A classification system for global wave energy resources based on multivariate clustering. *Appl Energy* 2020;262:114515.
- [55] Jung A, Baranov I. Basic principles of clustering methods. 2019, arXiv preprint arXiv:1911.07891.
- [56] Fraley C, Raftery A. MCLUST: Software for model-based cluster and discriminant analysis. *Dep Stat Univ Washington: Tech Rep* 1998;342:1312.
- [57] Scrucca L, Fraley C, Murphy TB, Raftery AE. Model-based clustering, classification, and density estimation using mclust in R. *Chapman and Hall/CRC*; 2023.
- [58] Jonkman J, Butterfield S, Musial W, Scott G. Definition of a 5-MW reference wind turbine for offshore system development. *Tech. rep., Golden, CO (United States: National Renewable Energy Lab.(NREL);* 2009.
- [59] Gilleland ME. Package 'ismev'. 2018.
- [60] Kharif C, Pelinovsky E, Slunyaev A. *Rogue waves in the ocean*. Springer Science & Business Media; 2008.
- [61] Dysthe K, Krogstad HE, Müller P. Oceanic rogue waves. *Annu Rev Fluid Mech* 2008;40(1):287–310.
- [62] Didenkulova E. Catalogue of rogue waves occurred in the world ocean from 2011 to 2018 reported by mass media sources. *Ocean & Coastal Management* 2020;188:105076.
- [63] Chun K, Wheeler H. An extreme analysis for the 2010 precipitation event at the south of Saskatchewan Prairie. *Glob Nest J* 2013;14:311–24.